

# Anticipatory Association for Indoor Visible Light Communications: Light, Follow Me!

Rong Zhang<sup>1</sup>, Senior Member, IEEE, Ying Cui<sup>1</sup>, Holger Claussen, Senior Member, IEEE,  
Harald Haas, Fellow, IEEE, and Lajos Hanzo<sup>1</sup>

**Abstract**—In this paper, a radically new anticipatory perspective is taken into account when designing the user-to-access point (AP) associations for indoor visible light communications (VLC) networks, in the presence of users' mobility and wireless-traffic dynamics. In its simplest guise, by considering the users' future locations and their predicted traffic dynamics, the novel anticipatory association prepares the APs for users in advance, resulting in an enhanced location- and delay-awareness. This is technically realized by our contrived design of an efficient approximate dynamic programming algorithm. More importantly, this paper is in contrast to most of the current research in the area of indoor VLC networks, where a static network environment was mainly considered. Hence, this paper is able to draw insights on the performance trade-off between delay and throughput in dynamic indoor VLC networks. It is shown that the novel anticipatory design is capable of significantly outperforming the conventional benchmarking designs, striking an attractive performance trade-off between delay and throughput. Quantitatively, the average system queue backlog is reduced from 15 to 8 [ms], when comparing the design advocated to the conventional benchmark at the per-user throughput of 100 [Mbps], in a  $15 \times 15 \times 5$  [m<sup>3</sup>] indoor environment associated with  $8 \times 8$  APs and 20 users walking at 1 [m/s].

**Index Terms**—VLC, user-association, dynamic programming, machine learning, hand-over, user-centric networking.

## I. INTRODUCTION

**V**ISIBLE Light Communications (VLC) constitutes a compelling technique of meeting the escalating wireless-traffic demands, as a new member in the beyond

Manuscript received December 15, 2016; revised July 31, 2017 and November 19, 2017; accepted January 16, 2018. Date of publication January 26, 2018; date of current version April 8, 2018. This work was supported in part by the EPSRC under Project EP/N004558/1 and Project EP/N023862/1 and in part by European Research Council's Advanced Fellow Grant. The work of Y. Cui was supported by the National Science Foundation of China under Grant 61401272 and Grant 61521062 and the Shanghai Key Laboratory under Grant STCSM15DZ2270400. The work of H. Haas was supported by the EPSRC through Established Career Fellowship under Grant EP/K008757/1. The data from the paper can be obtained from the University of Southampton ePrints research repository: 10.5258/SOTON/D0389. The associate editor coordinating the review of this paper and approving it for publication was M. S. Alouini. (Corresponding author: Lajos Hanzo.)

R. Zhang and L. Hanzo are with Southampton Wireless Group, School of Electronics and Computer Science, University of Southampton, Southampton SO17 1BJ, U.K. (e-mail: lh@ecs.soton.ac.uk).

Y. Cui is with the Department of Electronic Engineering, Shanghai Jiao Tong University, Shanghai 200240, China

H. Claussen is with the Small Cells Research, Bell Laboratories, Alcatel-Lucent, Dublin 15, Ireland

H. Haas is with the Li-Fi Research and Development Centre, Institute for Digital Communications, University of Edinburgh, Edinburgh EH8 9YL, U.K.

Color versions of one or more of the figures in this paper are available online at <http://ieeexplore.ieee.org>.

Digital Object Identifier 10.1109/TWC.2018.2797182

Fifth-Generation (5G) Heterogeneous Networks (HetNet) landscape [1]. There have been tremendous link-level achievements of VLC using state-of-the-art Light Emitting Diodes (LEDs) and Photo-Detectors (PDs) [2], sophisticated signal processing techniques [3] and advanced LED components [4]. The system-level studies<sup>1</sup> of VLC have also been rapidly developed for broadening its scope beyond point-to-point applications [5]. Recent advances have been partially inspired by numerous advanced Radio Frequency (RF) techniques. It is paramount however that these designs are suitably tailored for the specifics of VLC transceivers, propagation characteristics, illumination requirements, etc. Explicitly, straightforward adoption is completely unsuitable. Particularly, in indoor VLC, each Access Point (AP) constructs an 'atto-cell' with a few meters of radius confined by the coverage of light propagation [6]. Different from the RF regime, the number of APs may be higher than the number of users, resulting into ultra-dense networks [7], [8]. However, existing studies on indoor VLC were mainly focused on static network settings, while in this paper we study the challenging scenario of dynamic network settings, capturing both the users' mobility and wireless traffic dynamics.

When designing indoor VLC systems for supporting the users' mobility, the specific technique of associating the users with APs plays a crucial role, which requires *location-awareness*. Indeed, taking into account the users' geo-location information is both desirable and feasible, since there are important scenarios where the users' geo-locations are predefined or highly predictable, such as those of the robots and machines in warehouses, airports, museums, libraries, hospitals etc. In fact, there has been active research on indoor VLC positioning and tracking techniques [9], where the recent advances have achieved sub-centimetre accuracy [10], [11]. Furthermore, it is also desirable for the user-to-AP associations to have *delay-awareness*, so that to maintain queue stability for moving users with dynamic wireless traffic. Indeed, delay-aware system design has been a challenging and important subject [12]. Hence, significant research efforts have been dedicated to finding solutions for maintaining queue stability with the aid of e.g. Lyapunov optimisation [13] and machine

<sup>1</sup>Link-level studies of VLC refer to research aspects including but not limited to optical electronics and components; transceiver architectures; coding, modulation and dimming control; synchronisation, equalisation and estimation etc. By contrast, system-level studies of VLC include random and multiple access; interference management; resource allocation; user association and scheduling; mobility control etc.

learning [14] techniques. In fact, considering delay-awareness allows us to investigate the inherent trade-off between the average system queue backlog and the average per-user throughput of indoor VLC dynamic network settings.

In order to fully exploit the location- and delay-awareness, we conceive a novel *anticipatory* design principle by taking into account the anticipated users' mobility and wireless traffic dynamics when designing indoor VLC solutions [15]. Hence, anticipatory design constitutes an enhancement of the conventional location- and delay-aware designs with no foresight. To elaborate, prior research efforts have demonstrated the significant potential benefits of anticipatory design, through profiling the users' mobility pattern [16], link quality [17], traffic distribution [18] and social connection [19], etc. Sophisticated technical modelling methods, such as time-series analysis [20], classification [21], regression [22] as well as Bayesian inference solutions [23] have also been investigated, along with various mathematical optimisation methods [24]–[26]. These encouraging studies further consolidated our motivation to pursue anticipatory design for indoor VLC. In our anticipatory design, we assume the priori knowledge of the users' wireless-traffic distribution (not the exact packet arrivals) and perfect geo-locations. Instead of dealing with how to predict these quantities, our focus is on how to exploit this information in designing stable indoor VLC system.

*In this paper, we investigate indoor VLC in the context of dynamic network settings by adopting anticipatory design principles for formulating the association decisions in order to fully exploit both location- and delay-awareness.*

- We consider the Responsive Association (RA) benchmarking concept, where the associations are established by taking into account both the users' current geo-locations and their current queue backlog states. Furthermore, we consider the radical concept of Anticipatory Association (AA), where the associations are established by taking into account both the users' time-variant geo-locations and their evolving queue backlog states.
- We provide efficient solutions for both designs, relying on the approximate dynamic programming technique for solving the AA design problem. Beneficially, the AA design is capable of preparing the APs for handling the users' mobility by establishing anticipated connections around the users' movements. Hence, the AA design strikes an attractive performance trade-off between the average system queue backlog and the average per-user throughput.

To the best of our knowledge, this study is the first one characterising the delay versus throughput trade-offs for indoor VLC in the context of dynamic network settings. This is both timely and important, since future mobile networks aim at achieving both a short delay and a high throughput [27].

The rest of the paper is organised as follows. In Section II, we describe the channel model, the transmission model and the service model, which are then used for formulating our association design problems. In Section III, we provide efficient solutions to both the RA design problem and the

AA design problem, where the approximate dynamic programming method is formally introduced. Finally, we present numerical results for both the association designs in Section IV and we conclude our discourse in Section V.

## II. SYSTEM DESCRIPTION

Let us consider an indoor VLC environment relying on  $N$  APs uniformly installed on the ceiling at a height of  $H_t$ , where each AP is constituted by an array of  $L$  LEDs pointing vertically downwards and emitting the same optical power. These APs are used for communicating with  $K$  randomly distributed mobile users at a height of  $H_r$ , while at the same time providing illumination. The specific mobility model is introduced in Section IV. Each of these  $K$  mobile users generates wireless-traffic obeying a certain distribution. The specific wireless-traffic model is introduced in Section IV.

### A. Model Description

1) *Channel Model*: Since the users are on the move, their optical channels are also time-variant. At the  $t$ th timeslot, the optical channel between the  $k$ th user and the  $n$ th AP is constituted by both the direct Line-of-Sight (LoS) component and its reflections. Specifically, the LoS component  $h_{k,n}^{t,0}$  is given by [28]

$$h_{k,n}^{t,0} = \frac{(m_L + 1)A_0}{2\pi d^t d^t} \cos^{m_L}(\theta^t) \cos(\psi^t) f_{of}(\psi^t) f_{oc}(\psi^t), \quad (1)$$

where the Lambert index  $m_L = -1/\log_2[\cos(\phi_{1/2})]$  depends on the semi-angle  $\phi_{1/2}$  of the source at half-illumination. Furthermore,  $A_0$  is the physical area of the PD receiver,  $d^t$  is the distance between the  $k$ th user and the  $n$ th AP,  $\theta^t$  is the angle of irradiance from the  $n$ th AP and  $\psi^t$  is the angle of incidence at the  $k$ th user. Still referring to (1),  $f_{of}(\psi^t)$  and  $f_{oc}(\psi^t)$  denote the gains of the optical filter and of the optical concentrator employed, respectively. Furthermore,  $f_{oc}(\psi^t)$  can be written as

$$f_{oc}(\psi^t) = \begin{cases} n_r^2 / \sin^2(\psi^t) & \psi^t \leq \psi_F \\ 0 & \psi^t > \psi_F, \end{cases} \quad (2)$$

where  $\psi_F$  represents half of the receiver's Field-of-View (FoV) and  $n_r$  is the refractive index of a lens at the PD receiver.

With regards to the channel, we only consider the first reflection, since higher-order reflections are typically negligible. Explicitly, the first reflected component  $h_{k,n}^{t,1}$  is given by [28]

$$h_{k,n}^{t,1} = \sum_{\{v,u\}} \frac{\rho_r A_r d^t d^t}{d_{v,u,1}^2 d_{v,u,2}^t d_{v,u,2}^t} \cos(\alpha_{v,u}) \cos(\beta_{v,u}^t) h_{k,n}^{t,0}, \quad (3)$$

where  $d_{v,u,1}$  is the distance between the  $n$ th AP and the  $(v,u)$ th reflection point, and  $d_{v,u,2}^t$  is the distance between the  $(v,u)$ th reflection point and the  $k$ th user. Furthermore,  $\alpha_{v,u}$  and  $\beta_{v,u}^t$  denote the angle of incidence for the incoming light and the angle of irradiance for the outgoing light at the  $(v,u)$ th reflection point, having a tiny area of  $A_r$  and a reflectance factor of  $\rho_r$ . Furthermore, the pair of summations in (3) include all the reflections from the walls. Finally, the aggregated optical channel between the  $k$ th user and the

$n$ th AP is given by  $h_{k,n}^t = h_{k,n}^{t,0} + h_{k,n}^{t,1}$ , where we assume a single-tap channel response in this paper.

The optical channels' evolution due to the users' mobility also triggers the changes in the user-to-AP associations. More explicitly, at the  $t$ th timeslot, we let  $\mathcal{N}_k^t$  host the subset of APs associated with the  $k$ th user, where these subsets are mutually exclusive, i.e. we have  $\mathcal{N}_j^t \cap \mathcal{N}_k^t = \emptyset, \forall j \neq k$ . Similarly, we let  $\mathcal{N}_{-k}^t = \cup_{j \neq k} \mathcal{N}_j^t$  host the subset of APs associated with all but the  $k$ th user. We further let  $\mathcal{N}_{k,0}^t$  host the subset of APs having LoS connections with the  $k$ th user. Similarly, we let  $\mathcal{N}_0^t = \cup_k \mathcal{N}_{k,0}^t$  host the subset of APs having LoS connections with all users. In this paper, only those associations are established, where the LoS connections are present between the users and APs. Hence we have the relationship  $\mathcal{N}_k^t \subseteq \mathcal{N}_{k,0}^t$ .

2) *Transmission Model*: Naturally, the changes in user-to-AP associations consequently affect the service rates provided by the network for moving users. To this end, we consider the classic DC-biased OOFDM (DCO-OFDM) as our link-level transmission technique. Let  $\sigma_s^2$  denote the electronic power of the undistorted and unclipped DCO-OFDM signal. Owing to the LED's limited dynamic range, clipping may be imposed on the transmitted DCO-OFDM signal. Hence, we further let  $\sigma_c^2$  and  $\gamma_c$  denote the corresponding clipping noise power and clipping distortion factor, respectively. To elaborate, the clipping noise power  $\sigma_c^2$  is given by [29]

$$\sigma_c^2 = \sigma_A^2 - \sigma_B^2 - \gamma_c^2 \sigma_s^2, \quad (4)$$

where according to [29],  $\sigma_A^2$  is given in (5), as shown at the bottom of this page, and  $\sigma_B$  can be written as

$$\sigma_B = \sigma_s \left[ \frac{1}{\sqrt{2\pi}} \exp\left(\frac{\check{\epsilon}^2}{2}\right) + \check{\epsilon} - f_Q(\check{\epsilon})\check{\epsilon} + f_Q(\hat{\epsilon})\hat{\epsilon} \right]. \quad (6)$$

Here, we define  $\check{\epsilon} = (P_{min} - P_{DC})/\sigma_s$  and  $\hat{\epsilon} = (P_{max} - P_{DC})/\sigma_s$  as the normalised bottom and top clipping level, with an appropriate DC level of  $P_{DC}$  and the per-LED dynamic range of  $[P_{min}, P_{max}]$ . Furthermore, according to [29], the clipping distortion factor  $\gamma_c$  is given by  $\gamma_c = f_Q(\check{\epsilon}) - f_Q(\hat{\epsilon})$ , where  $f_Q$  represents the standard  $Q$ -function.

Hence, at the  $t$ th timeslot and a particular user-to-AP association, the downlink service rate  $r_k^t$  of the  $k$ th user can be written as

$$r_k^t = \frac{B}{2} \log_2 \left[ 1 + \frac{\gamma_c^2 \sigma_s^2 (\sum_{n \in \mathcal{N}_k^t} h_{k,n}^t)^2}{\sigma_c^2 (\sum_{n \in \mathcal{N}_k^t} h_{k,n}^t)^2 + I_k^t + \sigma^2} \right], \quad (7)$$

where the interference term in (7) can be formulated as

$$I_k^t = (\sigma_A^2 - \sigma_B^2) (\sum_{n \in \mathcal{N}_{-k}^t} h_{k,n}^t)^2. \quad (8)$$

Furthermore, the noise term in (7) includes both the shot noise and the thermal noise, which can be modelled as zero-mean complex-valued Additive White Gaussian Noise (AWGN) with an equivalent variance of  $\sigma^2 = BN_0/L^2$ , where  $B$  is the modulation bandwidth and  $N_0 \approx 10^{-22}$  A<sup>2</sup>/Hz [2] is the noise

power spectral density. Finally, since the DCO-OFDM signal is real-valued, the information rate  $r_k^t$  of (7) is also halved.

3) *Service Model*: In addition to the users' mobility dynamics, we also consider wireless traffic dynamics, where these two types of dynamics together result into time-variant queues. Explicitly, at the  $t$ th timeslot, the  $k$ th user has a queue backlog of  $q_k^t$  with a service rate of  $r_k^t$ . There is also a random packet arrival of  $a_k^t$  following a certain wireless-traffic distribution, with  $\eta = \mathbb{E}[a_k^t], \forall k$  representing the user's average throughput. Hence, the  $k$ th user's queue backlog at the  $t$ th timeslot is the remaining queue backlog at the  $(t-1)$ th timeslot after being served, whilst also taking into account the new packet arrivals at the  $(t-1)$ th timeslot. Mathematically, the  $k$ th user's queue backlog expressed in terms of delay evolves according to

$$q_k^t = (q_k^{t-1} - r_k^{t-1} \delta / \eta)^+ + a_k^{t-1} \delta / \eta, \quad (9)$$

where  $(\cdot)^+$  represent the operator returning the maximum between its argument and zero, while  $\delta$  is the timeslot duration. It is plausible that the dynamic evolution of the queues is depended on the random packet arrivals and the time-variant service rates, which are directly related to the user-to-AP associations, that in turn are subject to the users' mobility dynamics. Hence, the appropriate design of user-to-AP associations is of utmost importance.

Let us now introduce  $x_{k,n}^t \in \{0, 1\}$  to indicate the association between the  $k$ th user and the  $n$ th AP at the  $t$ th timeslot, which is one if there is an association and zero otherwise. Hence, the service rate  $r_k^t$  of (7) can be represented alternatively in terms of  $x_{k,n}^t$  as

$$r_k^t = \frac{B}{2} \sum_n \frac{x_{k,n}^t}{\|\mathbf{x}_k^t\|^2} \log_2 \left[ 1 + \frac{\gamma_c^2 \sigma_s^2 (\mathbf{x}_k^t \mathbf{h}_k^t)^2}{\sigma_c^2 (\mathbf{x}_k^t \mathbf{h}_k^t)^2 + I_k^t + \sigma^2} \right], \quad (10)$$

where the interference term in (10) is given by

$$I_k^t = (\sigma_A^2 - \sigma_B^2) (\sum_{j \neq k} \mathbf{x}_j^t \mathbf{h}_k^t)^2. \quad (11)$$

Here,  $\mathbf{x}_k^t = [x_{k,1}^t, \dots, x_{k,N}^t]$  denotes the  $k$ th user's association vector and  $\mathbf{h}_k^t = [h_{k,1}^t, \dots, h_{k,N}^t]^T$  denotes the  $k$ th user's channel vector, with  $(\cdot)^T$  being the vector transpose. Now, we are fully prepared to formulate our design problems.

## B. Problem Formulation

When experiencing both user mobility and dynamic wireless-traffic, a salient design problem in indoor VLC is to determine the specific user-to-AP associations that are capable of maintaining queue stability, where the multi-user queues are deemed to be stable if they have a finite average queue backlog for the entire system. Hence, a particular association design is deemed superior to another, if it strikes a better trade-off between the average system queue backlog and the average per-user throughput. In this light, we consider both the RA design and the AA design, with both location- and delay-awareness.

$$\sigma_A^2 = \sigma_s^2 \left[ f_Q(\check{\epsilon}) - f_Q(\hat{\epsilon}) + \frac{\check{\epsilon}}{\sqrt{2\pi}} \exp\left(\frac{-\check{\epsilon}^2}{2}\right) - \frac{\hat{\epsilon}}{\sqrt{2\pi}} \exp\left(\frac{-\hat{\epsilon}^2}{2}\right) + \check{\epsilon}^2 - f_Q(\check{\epsilon})\check{\epsilon}^2 + f_Q(\hat{\epsilon})\hat{\epsilon}^2 \right], \quad (5)$$

1) *Responsive Association*: One of the throughput-optimal and delay-aware design principles that guarantees queue stability in single-hop networks is known as the Largest Weighted Delay First (LWDF) [30] technique. Hence, in this paper, we adopt it as our benchmarking RA design, while referring the motivated readers to [30] for further details on the underlying theory. More explicitly, the objective of the RA design is to obtain the optimal association decisions between the  $K$  users and  $N$  APs in order to maximise the weighted sum rate *at the current timeslot*, where the weight is the *current* queue backlog of each user. Mathematically, the RA design problem can be formulated as

$$\mathcal{P}_{RA} = \max_{\{x_{k,n}^t, \forall k,n\}} \sum_k q_k^t r_k^t, \quad (12)$$

$$\text{s.t. } \sum_k x_{k,n}^t \leq 1 \quad \forall n, \quad (13)$$

$$\sum_n x_{k,n}^t \leq N_k \quad \forall k, \quad (14)$$

$$x_{k,n}^t \in \{0, 1\} \quad \forall k, n \in \mathcal{N}_{k,0}^t, \quad (15)$$

$$x_{k,n}^t = 0 \quad \forall k, n \notin \mathcal{N}_{k,0}^t. \quad (16)$$

Observe that in (12), the objective function is designed for ensuring that users having higher queue backlog would have higher priorities, reflecting the LWDF design principle. Furthermore, constraint (13) requires that an AP can only serve at most one user, in the spirit of Time Division Multiple Access (TDMA), while constraint (14) ensures that the  $k$ th user can only be served by at most  $N_k$  APs, where  $1 \leq N_k \leq |\mathcal{N}_{k,0}^t|$  is a pre-defined integer. Finally, constraint (16) reflects the fact that only the LoS component is used for determining the association.

2) *Anticipatory Association*: In contrast to the RA design, the objective of the AA design is to obtain the optimal association decisions between the  $K$  users and  $N$  APs in order to maximise the weighted sum rate *for the duration of several future timeslots*, where the weight is represented by the *evolving* queue backlog of each user over several future timeslots. Conceptually, the proposed AA design may be viewed as an enhanced version of the LWDF design principle, which is endowed with a look-ahead capability. Mathematically, the AA design problem can be formulated as

$$\mathcal{P}_{AA} = \max_{\{x_{k,n}^{t_w}, \forall w,k,n\}} \mathbb{E} \left[ \sum_w \sum_k q_k^{t_w} r_k^{t_w} \right], \quad (17)$$

$$\text{s.t. } \sum_k x_{k,n}^{t_w} \leq 1 \quad \forall w, n, \quad (18)$$

$$\sum_n x_{k,n}^{t_w} \leq N_k \quad \forall w, k, \quad (19)$$

$$x_{k,n}^{t_w} \in \{0, 1\} \quad \forall w, k, n \in \mathcal{N}_{k,0}^{t_w}, \quad (20)$$

$$x_{k,n}^{t_w} = 0 \quad \forall w, k, n \notin \mathcal{N}_{k,0}^{t_w}, \quad (21)$$

where  $t_w = t + w - 1$  and  $w \in [1, W]$  with  $W$  being the total number of timeslots considered in the AA design. Furthermore, the expectation in (17) reflects the stochastic

nature of the packet arrival process, which is assumed to be an independent and identically distributed (i.i.d.) process having a known distribution. Finally, the constraints of the AA design problem follow similar interpretations to those of the RA design problem discussed previously.

*Remark 1*: It is plausible that the AA design problem defined in (17) provides a higher degree of system optimisation flexibility, than the RA design problem defined in (12). This is because the knowledge of the users' future geo-locations, which also determine their potential service rates, together with the users' wireless-traffic distribution may be taken into account in the AA design. Intuitively, the users who are about to experience high-quality links may be delayed, while serving those users promptly, who are experiencing or about to experience weak links. Hence, the anticipatory design principle is capable of exploiting the beneficial foresight of location- and delay-awareness.

*Remark 2*: Conventional predictive handover used in mobile telephony normally deals with the problem of early or late handover trigger, which is achieved by adjusting the handover trigger according to the a priori knowledge of the target AP/router [31], [32]. It is a pure handover decision between a link about to be relinquished and another to be established from the user's point of view. By contrast, in this paper, we consider the user association problem, where a particular user may be associated with multiple APs at the same time. Hence, the updated associations would be established amongst multiple APs, which means that there are multiple links to be relinquished and to be set-up from the user's point of view. Even more intriguing is that the (updated) association decisions are coupled with those of other users, where these couplings are strong in the ultra-dense network environment considered in this paper. These particulars make our problem much more challenging, yet interesting both conceptually and technically. Our methodology may also be applied in RF small-cell networks, including within the context of phantom cell arrangements.

### III. METHODOLOGY

Let us now elaborate on the methodology used for solving both the RA design problem and the AA design problem.

#### A. Responsive Association

1) *Transformation*: The RA design problem defined in (12) is *strongly* coupled, since the decision variables  $x_{k,n}^t$  are all coupled through both the objective function and the constraints. Substituting (10) into (12) reveals that the decision variable  $x_{k,n}^t$  is closely related to both the  $k$ th user's association vector  $\mathbf{x}_k^t$  and the other users' association vectors  $\mathbf{x}_j^t, \forall j \neq k$ . Hence, we pursue a conservative approach by considering the worst-case maximum interference  $\tilde{I}_k^t$  imposed on the  $k$ th user, which is given by

$$\tilde{I}_k^t = (\sigma_A^2 - \sigma_B^2)(\mathbf{e}^t \mathbf{h}_k^t - \mathbf{x}_k^t \mathbf{h}_k^t)^2, \quad (22)$$

where  $\mathbf{e}^t = [e_1^t, \dots, e_N^t]$  with  $e_n^t = 1, \forall n \in \mathcal{N}_0^t$  and  $e_n^t = 0$  otherwise. Correspondingly, the original service rate  $r_k^t$  of (10) is replaced by the associated lower bound of the service rate,

which is given by

$$\tilde{r}_k^t = \frac{B}{2} \sum_n \frac{x_{k,n}^t}{\|\mathbf{x}_k^t\|^2} \log_2 \left[ 1 + \frac{\gamma_c^2 \sigma_s^2 (\mathbf{x}_k^t \mathbf{h}_k^t)^2}{\sigma_c^2 (\mathbf{x}_k^t \mathbf{h}_k^t)^2 + \tilde{I}_k^t + \sigma^2} \right]. \quad (23)$$

It is clear that  $x_{k,n}^t$  and  $\mathbf{x}_j^t, \forall j \neq k$  has now been decoupled in (23). Hence, the RA design problem can be redefined as

$$\begin{aligned} \tilde{\mathcal{P}}_{RA} = \max_{\{x_{k,n}^t, \forall k,n\}} & \sum_k q_k^t \tilde{r}_k^t, \\ \text{s.t.} & (13), (14), (15), (16), \end{aligned} \quad (24)$$

where we next discuss its solution for both the special case of  $N_k = 1, \forall k$  and the general case of  $N_k \geq 1, \forall k$ .

2) *Optimisation*: Setting  $N_k = 1, \forall k$  in constraint (14) results into the scenario of single-AP association, where (24) can be explicitly expanded as

$$\begin{aligned} \tilde{\mathcal{P}}_{RA}^s = \max_{\{x_{k,n}^t, \forall k,n\}} & \sum_k q_k^t \tilde{r}_k^{t,s}, \\ \text{s.t.} & (13), (14), (15), (16). \end{aligned} \quad (25)$$

Here,  $\tilde{r}_k^{t,s}$  is the conservative service rate when single-AP association is employed for all users, which is given by

$$\tilde{r}_k^{t,s} = \frac{B}{2} x_{k,n}^t \log_2 \left[ 1 + \frac{\gamma_c^2 \sigma_s^2 (h_{k,n}^t)^2}{\sigma_c^2 (h_{k,n}^t)^2 + \tilde{I}_k^{t,s} + \sigma^2} \right], \quad (26)$$

where the interference term in (26) when single-AP association is employed for all users is given by

$$\tilde{I}_k^{t,s} = (\sigma_A^2 - \sigma_B^2) (\mathbf{e}^t \mathbf{h}_k^t - h_{k,n}^t)^2. \quad (27)$$

It is plausible that the problem defined in (25) is a classic binary linear programming problem. Since an efficient solution exists, we do not elaborate on it further in this contribution.

On the other hand, setting  $N_k \geq 1, \forall k$  in constraint (14) results into the general scenario of multi-AP association, which may also be referred to as channel *bonding*. However, its solution is not as straightforward as that of the single-AP association scenario. To solve this problem, we let  $\mathcal{K}_v^t$  host the subset of users having the capability of multi-AP association at the  $t$ th timeslot. For a particular user  $j \in \mathcal{K}_v^t$ , we let  $\mathcal{C}_{j,m}^t$  host all the combinations of  $m$ -AP association with  $m \in \{2, 3, \dots, N_j\}$ . For each of these combinations, we create a corresponding virtual user, where we introduce  $y_{c_j^m, n}^t \in \{0, 1\}$  to indicate the association between the  $c_j^m$ th virtual user and the  $n$ th AP at the  $t$ th timeslot. Similarly, we use  $\mathbf{y}_{c_j^m}^t$  to denote the  $c_j^m$ th virtual user's association vector at the  $t$ th timeslot. Hence, (24) can be transformed into

$$\tilde{\mathcal{P}}_{RA}^b = \max_{\{\mathbf{x}_k^t, \mathbf{y}_{c_j^m}^t, z_{c_j^m}^t\}} \sum_k q_k^t \tilde{r}_k^{t,s} + \sum_j \sum_m \sum_{c_j^m} q_j^t \tilde{r}_{c_j^m}^{t,b}, \quad (28)$$

s.t. (15), (16),

$$\sum_k x_{k,n}^t + \sum_j \sum_m \sum_{c_j^m} y_{c_j^m, n}^t \leq 1 \quad \forall n, \quad (29)$$

$$\sum_n x_{k,n}^t \leq 1 \quad \forall k, \quad (30)$$

$$\sum_n x_{j,n}^t + \sum_{c_j^m} \sum_n y_{c_j^m, n}^t \leq m \quad \forall j, m, \quad (31)$$

$$\sum_n y_{c_j^m, n}^t + z_{c_j^m}^t m = m \quad \forall j, m, c_j^m, \quad (32)$$

$$z_{c_j^m}^t \in \{0, 1\} \quad \forall j, m, c_j^m, \quad (33)$$

$$y_{c_j^m, n}^t \in \{0, 1\} \quad \forall j, m, c_j^m, n, \quad (34)$$

where  $\tilde{r}_{c_j^m}^{t,b} = \tilde{r}_j^t(\mathbf{x}_j^t = \mathbf{y}_{c_j^m}^t)$  is the conservative service rate for the  $c_j^m$ th virtual user when multi-AP association is used. To elaborate, constraint (29) requires that an AP can only serve at most one user, while constraints (30) and (31) jointly require that the users supporting single-AP association can only be served by at most one AP and users having  $m$ -AP association can only be served by at most  $m$  APs. Finally, constraint (32) requires that the  $c_j^m$ th virtual user can either be served by  $m$  APs or not be served at all. By introducing the concept of virtual users, it is plausible that the problem defined in (28) becomes a classic binary linear programming problem, for which efficient solutions exist. Following the optimisation, we assign  $\mathbf{x}_j^t = \mathbf{y}_{c_j^m}^t$ , if the  $j$ th user's  $c_j^m$ th multi-AP association was finally determined.

## B. Anticipatory Association

1) *Transformation*: It is clear that the AA design problem defined in (17) is also *strongly* coupled. Similar to the transformation carried out for the RA design, we use the conservative service rate  $\tilde{r}_k^t$  of (23), rather than the original service rate  $r_k^t$  of (10), when dealing with the AA design problem. Furthermore, we define the *action* of the  $k$ th user at the  $t_w$ th timeslot as  $\tilde{r}_k^{t_w}$ , which is independent of the other users' actions. According to (23), the conservative service rate  $\tilde{r}_k^{t_w}$  is a function of the  $k$ th user's association vector  $\mathbf{x}_k^{t_w}$ . Hence, by enumerating all possible combinations of the  $k$ th user's association vector, the corresponding *action set*  $\mathcal{A}_k^{t_w}$  can be created.

As a benefit of using the conservative service rate  $\tilde{r}_k^{t_w}$ , when  $w \geq 2$ , the  $k$ th user's queue backlog evolves according to

$$\tilde{q}_k^{t_w} = (\tilde{q}_k^{t_{w-1}} - \tilde{r}_k^{t_{w-1}} \delta / \eta)^+ + a_k^{t_{w-1}} \delta / \eta, \quad (35)$$

where  $\tilde{q}_k^{t_1} = q_k^t$  is the  $k$ th user's initial queue backlog at the  $t$ th timeslot. However, the continuous-valued queue backlog of  $\tilde{q}_k^{t_w}$  cannot be directly used for the dynamic programming aided methods to be employed next. Hence, we introduce a discrete-valued queue backlog of  $s_k^{t_w} \in \mathcal{S}$ , where  $\mathcal{S}$  hosts the quantised queue backlog lengths capped at  $q_\Delta$  having the discretisation granularity of  $\Delta$ . Hereafter,  $\mathcal{S}$  is referred to as the *state set*, and each level in  $\mathcal{S}$  is referred to as a *state*. Hence, when  $w \geq 2$ , the  $k$ th user's discrete-valued queue backlog evolves according to

$$s_k^{t_w} = \lfloor \min[(s_k^{t_{w-1}} - \tilde{r}_k^{t_{w-1}} \delta / \eta)^+ + a_k^{t_{w-1}} \delta / \eta, q_\Delta] \rfloor, \quad (36)$$

where  $s_k^{t_1} = \lfloor \min[q_k^t, q_\Delta] \rfloor$  is the  $k$ th user's starting queue backlog at the  $t$ th timeslot and  $\lfloor \cdot \rfloor$  is the quantisation operation.

After introducing the above-mentioned concept of action and state, the AA design problem can be redefined as

$$\begin{aligned} \tilde{\mathcal{P}}_{AA} = \max_{\{\tilde{r}_k^{t_w}, \forall w,k\}} & \mathbb{E} \left[ \sum_w \sum_k R_k^{t_w} \right], \\ \text{s.t.} & (18), (20), (21), \end{aligned} \quad (37)$$

where  $R_k^{t_w} = s_k^{t_w} \tilde{r}_k^{t_w}$  represents the  $k$ th user's reward at the  $t_w$ th timeslot. Note that constraint (19) is dropped here, since the enumeration of the  $k$ th user's actions ensures that constraint (19) will always be satisfied. To elaborate a little further, (37) resorts to finding the best actions  $\tilde{r}_k^{t_w}$  of all users throughout all timeslots so as to maximise the sum of each user's reward  $R_k^{t_w}$  over all timeslots in a stochastic sense, where each user's state  $s_k^{t_w}$  evolves according to (36).

However, directly solving (37) may be excessive at the current computing power. Let  $\mathbf{s}^{t_w} = \{s_k^{t_w}, \forall k\}$  and  $\tilde{\mathbf{r}}^{t_w} = \{\tilde{r}_k^{t_w}, \forall k\}$  denote the system states and system actions at the  $t_w$ th timeslot, respectively. Assuming that each user has the same number of actions throughout the timeslots, i.e. we have  $|\mathcal{A}_k^{t_w}| = |\mathcal{A}|, \forall w, k$ , then there is an unmanageable total number of  $|\mathcal{S}|^K$  system states and  $|\mathcal{A}|^K$  system actions at each timeslot. Unfortunately, these system states and system actions also expand exponentially in time, hence we resort to dynamic programming in order to circumvent the excessive growth in complexity [33], [34].

2) *Approximation*: In dynamic programming, we let  $J(\mathbf{s}^{t_1})$  denote the value of (37), which can be obtained by recursively solving the so-called Bellman equation, commencing from the  $t_W$ th timeslot. More explicitly, the Bellman equation [33] at the  $t_w$ th timeslot can be written as

$$J(\mathbf{s}^{t_w}) = \max_{\tilde{\mathbf{r}}^{t_w}} \sum_k R_k^{t_w} + \bar{J}(\mathbf{s}^{t_{w+1}})_{\mathbf{s}^{t_w}, \tilde{\mathbf{r}}^{t_w}}, \quad (38)$$

s.t. (18), (20), (21),

where  $\bar{J}(\mathbf{s}^{t_{w+1}})_{\mathbf{s}^{t_w}, \tilde{\mathbf{r}}^{t_w}}$  is the expected value at the  $t_{w+1}$ th timeslot of the immediate future, conditioned on the system states and system actions at the current  $t_w$ th timeslot and its value is zero at the dummy  $t_{W+1}$  timeslot. The typical approach invoked for recursively solving (38) requires either policy iteration or value iteration, both of which suffer from the *curse of dimensionality*. This is because both the number of system states and the number of system actions at each timeslot is exponential in the number of users  $K$ , owing to the coupling imposed by constraint (18). Fortunately, a closer look at (38) reveals that this is a *weakly* coupled dynamic programming problem [35], hence we exploit its structural property for developing an approximate dynamic programming method [36].

Formally, we aim to relax the constraint (18) by attaching Lagrange multipliers to (38). Let us define the Lagrange multipliers at the  $t_w$ th timeslot as  $\boldsymbol{\lambda}^{t_w} = \{\lambda_n^{t_w}, \forall n\}$ . Hence, the relaxed Bellman equation at the final  $t_W$ th timeslot can be written as

$$\begin{aligned} \mathcal{L}(\mathbf{s}^{t_w}, \boldsymbol{\lambda}^{t_w}) &= \max_{\tilde{\mathbf{r}}^{t_w}} \sum_k (R_k^{t_w} - \sum_n \lambda_n^{t_w} x_{k,n}^{t_w}) + \sum_n \lambda_n^{t_w} \\ &= \sum_k (\max_{\tilde{r}_k^{t_w}} R_k^{t_w} - \sum_n \lambda_n^{t_w} x_{k,n}^{t_w}) + \sum_n \lambda_n^{t_w} \\ &= \sum_k \mathcal{L}_k(s_k^{t_w}, \boldsymbol{\lambda}^{t_w}) + \sum_n \lambda_n^{t_w}. \end{aligned} \quad (39)$$

Let us also define the Lagrange multipliers ranging from the  $t_w$ th timeslot to the  $t_W$ th timeslot as  $\boldsymbol{\lambda}^{t_w, W} = \{\boldsymbol{\lambda}^{t_w}, w' \in [w, W]\}$ . Then reasoning by induction from (39), the relaxed

Bellman equation at the  $t_w$ th timeslot can be written as

$$\mathcal{L}(\mathbf{s}^{t_w}, \boldsymbol{\lambda}^{t_w, W}) = \sum_k \mathcal{L}_k(s_k^{t_w}, \boldsymbol{\lambda}^{t_w, W}) + \sum_{w'} \sum_n \lambda_n^{t_w}, \quad (40)$$

where explicitly we have

$$\begin{aligned} \mathcal{L}_k(s_k^{t_w}, \boldsymbol{\lambda}^{t_w, W}) \\ = \max_{\tilde{r}_k^{t_w}} R_k^{t_w} - \sum_n \lambda_n^{t_w} x_{k,n}^{t_w} + \bar{\mathcal{L}}_k(s_k^{t_{w+1}}, \boldsymbol{\lambda}^{t_{w+1}, W})_{s_k^{t_w}, \tilde{r}_k^{t_w}}. \end{aligned} \quad (41)$$

Here  $\bar{\mathcal{L}}_k(s_k^{t_{w+1}}, \boldsymbol{\lambda}^{t_{w+1}, W})_{s_k^{t_w}, \tilde{r}_k^{t_w}}$  is the expected value after relaxation at the  $t_{w+1}$ th timeslot of the immediate future, conditioned on the system states and system actions at the current  $t_w$ th timeslot and its value is zero at the dummy  $t_{W+1}$ th timeslot. It is now plausible that the above relaxation results in  $K$  small sub-problems of (41) at each timeslot and for each system state.

As a benefit of relaxation, the *dual* problem of the Bellman equation  $J(\mathbf{s}^{t_w})$  at the  $t_w$ th timeslot can be written as

$$\mathcal{L}(\mathbf{s}^{t_w}) = \min_{\boldsymbol{\lambda}^{t_w, W}} \mathcal{L}(\mathbf{s}^{t_w}, \boldsymbol{\lambda}^{t_w, W}), \quad (42)$$

where according to standard Lagrangian theory, (42) is convex and we have the relationship of  $\mathcal{L}(\mathbf{s}^{t_w}) \geq J(\mathbf{s}^{t_w})$ . Recall that our goal was to solve the Bellman equation  $J(\mathbf{s}^{t_1})$  at the  $t_1$ th timeslot, but now we resort to solving its *dual* problem of

$$\mathcal{L}(\mathbf{s}^{t_1}) = \min_{\boldsymbol{\lambda}^{t_1, W}} \mathcal{L}(\mathbf{s}^{t_1}, \boldsymbol{\lambda}^{t_1, W}). \quad (43)$$

This approach follows the design principle of the so-called approximate dynamic programming, which has been found in diverse applications [37]–[40].

3) *Solution*: At first glance, the linear programming representation of (43) can be written as

$$\mathcal{L}(\mathbf{s}^{t_1}) = \min_{\{\boldsymbol{\lambda}^{t_1, W}, \boldsymbol{\mu}\}} \sum_k \mu_k(s_k^{t_1}) + \sum_w \sum_n \lambda_n^{t_w}, \quad (44)$$

$$\begin{aligned} \text{s.t. } \mu_k(s_k^{t_w}) &\geq R_k^{t_w} - \sum_n \lambda_n^{t_w} x_{k,n}^{t_w} + \bar{\mu}_k(s_k^{t_{w+1}})_{s_k^{t_w}, \tilde{r}_k^{t_w}} \\ &\forall w, k, s_k^{t_w}, \tilde{r}_k^{t_w}, \end{aligned} \quad (45)$$

$$\lambda_n^{t_w} \geq 0 \quad \forall w, n, \quad (46)$$

where  $\boldsymbol{\mu} = \{\mu_k(s_k^{t_w}), \forall w, k, s_k^{t_w}\}$  hosts all of the auxiliary decision variables and  $\bar{\mu}_k(s_k^{t_{w+1}})_{s_k^{t_w}, \tilde{r}_k^{t_w}}$  is the expected value of the auxiliary decision variable at the  $t_{w+1}$ th timeslot of the immediate future, conditioned on the system states and system actions at the current  $t_w$ th timeslot and its value is zero at the dummy  $t_{W+1}$ th timeslot. Although (44) is in an elegant formulation, the underlying problem only remains tractable for small system settings. In a reasonable-sized system setting of  $N = 8 \times 8$  APs,  $K = 20$  users,  $W = 5$  timeslots,  $|\mathcal{S}| = 10$  states and  $|\mathcal{A}_k^{t_w}| = |\mathcal{A}| = 4, \forall w, k$  actions, there is a total of  $W(K|\mathcal{S}| + N) = 1320$  decision variables and  $WK|\mathcal{S}||\mathcal{A}| = 4000$  constraints involved in the problem formulated in (44), where a practical solution is indeed necessary.

Hence, we employ the classic sub-gradient based algorithm in order to obtain  $\mathcal{L}(\mathbf{s}^{t_1})$ . Explicitly, the sub-gradient based algorithm iteratively updates  $\boldsymbol{\lambda}^{t_1, W}$  according to

$$\boldsymbol{\lambda}^{t_1, W}(\tau + 1) = [\boldsymbol{\lambda}^{t_1, W}(\tau) + \boldsymbol{\epsilon} \mathbf{g}(\tau)]^+, \quad (47)$$

where  $\tau$  is the iteration index and  $\mathbf{g}(\tau)$  is the sub-gradient, which is given by

$$\mathbf{g}(\tau) = \nabla \mathcal{L}[\mathbf{s}^{t_1}, \boldsymbol{\lambda}^{t_1, w}(\tau)]. \quad (48)$$

In this study, we estimate the sub-gradient  $\mathbf{g}(\tau)$  empirically. For a given  $\boldsymbol{\lambda}^{t_1, w}(\tau)$ , we can readily obtain the corresponding chosen actions of  $\tilde{r}_k^{t_1, w}$  for all users and on all timeslots. This can be achieved by backwards recursion on the relaxed Bellman equation of (40), with its component equation (41) being efficiently evaluated at each recursion. These actions are then used for determining the estimated sub-gradient. Still referring to (47), the positive step size of  $\epsilon$  is given by

$$\epsilon = \frac{\min_{\tau' < \tau} \mathcal{L}[\mathbf{s}^{t_1}, \boldsymbol{\lambda}^{t_1, w}(\tau')] - \mathcal{L}[\mathbf{s}^{t_1}, \boldsymbol{\lambda}^{t_1, w}(\tau)]}{\|\mathbf{g}(\tau)\|^2}. \quad (49)$$

Finally, the sub-gradient based algorithm terminates, when  $\mathbf{g}(\tau)$  is deemed to be sufficiently small. The exact complexity of the sub-gradient based algorithm is difficult to quantify owing to its iterative nature. However, at each iteration, the backwards recursion on (40) requires  $WK|\mathcal{S}|$  evaluations of (41), which can be solved efficiently, namely at a linear complexity of  $\mathcal{O}(|\mathcal{A}_k^{t_1, w}|)$ . Hence, the sub-gradient based algorithm is indeed appropriate for practical sized problems. For better clarification, a pseudo-code is included in Algorithm 1.

---

**Algorithm 1** ADP

---

```

1: input  $\{\mathcal{A}_k^{t_1, w}, \forall k, t_w\}$ , initialise  $\boldsymbol{\lambda}^{t_1, w}(\tau = 1)$  and  $\varsigma$ 
2: for  $\tau = 1, 2, \dots$  do
3:   backwards recursion (40)  $\rightarrow \mathcal{L}[\mathbf{s}^{t_1}, \boldsymbol{\lambda}^{t_1, w}(\tau)]$ 
4:   evaluate (48)  $\rightarrow \mathbf{g}(\tau)$ 
5:   if  $\mathbf{g}(\tau) \leq \varsigma$  then
6:      $\boldsymbol{\lambda}^{t_1, w} = \boldsymbol{\lambda}^{t_1, w}(\tau)$ 
7:     break
8:   else
9:     evaluate (49)  $\rightarrow \epsilon$ 
10:    evaluate (47)  $\rightarrow \boldsymbol{\lambda}^{t_1, w}(\tau + 1)$ 
11:   end if
12: end for
13: evaluate  $J(\mathbf{s}^{t_1}) \approx \mathcal{L}(\mathbf{s}^{t_1}) = \mathcal{L}(\mathbf{s}^{t_1}, \boldsymbol{\lambda}^{t_1, w})$ 

```

---

#### IV. NUMERICAL RESULTS

We now characterise the performance of the average system queue backlog versus the average per-user throughput, for both of our association designs, under different parameter settings.

##### A. Settings

We considered a  $15 \times 15 \times 5$  [m<sup>3</sup>] indoor environment associated with  $N = 8 \times 8$  APs uniformly located on the ceiling. We set the optical power to  $P_o = 24.5$  [mW] for satisfying the illumination requirements of  $[\mathcal{I}_{min}, \mathcal{I}_{max}, \mathcal{I}_{avg}] = [200, 800, 600]$  [lm], where we define the minimum illumination requirement as  $\mathcal{I}_{min}$ , the maximum illumination requirement as  $\mathcal{I}_{max}$  and the average illumination requirement as  $\mathcal{I}_{avg}$ . Hence, we have the electronic power of  $\sigma_s^2 \approx 0.75$  [mW] corresponding to the DC level of  $P_{DC} = 22.5$  [mW], where the optical to electronic power conversion is discussed in Appendix.

TABLE I  
LIST OF COMMON PARAMETER SETTINGS

LED-related Parameters	
Semi-angle at half-illumination $\phi_{1/2}$	60°
Gain of optical filter $f_{of}(\psi)$	1
Physical area for a PD receiver $A_{PD}$	1 [cm <sup>2</sup> ]
Refractive index $n_r$	1.5
Reflection efficiency $\rho$	0.75
Optical power to luminous flux conversion factor $\xi$	2.1 [mW/lm]
Height of AP $H_t$	2.5 [m]
Height of user $H_r$	0.85 [m]
LED min optical power $P_{min}$	5 [mW]
LED max optical power $P_{max}$	50 [mW]
LED array per AP $L$	15 × 15

The classic random waypoint mobility model was adopted for users randomly distributed in the room, with a constant speed at  $v$  [m/s], walking duration from 2 to 5 [s], pausing duration from 0 to 2 [s] and walking direction spanning 360°. Each timeslot was set to  $\delta = 1$  [ms] and 10 independent snapshots of 30 [s] moving segments were recorded, where each snapshot was averaged over 50 Bernoulli distributed random packet arrivals with a mean of  $p$  and we set  $q_\Lambda = 5$  [ms].

The standard parameter settings used in our simulations were as follows: number of users  $K = 20$ , Bernoulli mean  $p = 0.5$ , maximum number of APs per-user  $N_k = 1, \forall k$ , modulation bandwidth  $B = 25$  MHz, half of the FoV  $\psi_F = 45^\circ$ , moving speed  $v = 1$  [m/s], prediction window size  $W = 10$  and discretisation granularity  $\Delta = 0.5$  [ms]. In the following, we investigate each of these parameters separately, whilst keeping all the other parameters unchanged. Finally, the remaining common parameter settings are listed in Table I.

##### B. Observations

1) *Effect of Number of Users*: The left subplot of Fig. 1 shows the effect of the number of users on the average system queue backlog versus the average per-user throughput, for both the RA design and the AA design. It is clear that for both user number settings of  $K = 20$  and  $K = 30$ , the AA design achieves a consistently shorter average system queue backlog than that of the RA design across all values of the per-user average throughput. Importantly, for both user number settings, the difference between the RA design and the AA design in the average system queue backlog substantially increases upon increasing the average per-user throughput. Quantitatively, for both user number settings and when supporting an average per-user throughput of 100 Mbps, the AA design results in about half of the average system queue backlog of that of the RA design, although their difference is only marginal when supporting the reduced average per-user throughput of 50 Mbps. Indeed, when increasing the average per-user throughput, the corresponding average system queue backlog increases much faster in the RA design than in the AA design, for both user number settings. Finally, for both the RA design and the AA design, the higher the number of users, the more system resources are required and the higher the average system queue backlog becomes.

2) *Effect of Field of View*: The right subplot of Fig. 1 shows the effect of the FoV on the average system queue

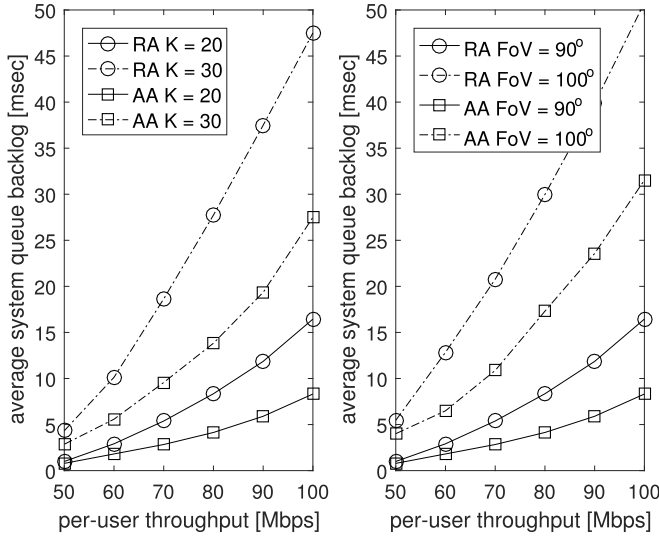


Fig. 1. The effect of number of users (left) and the effect of field of view (right) on the performance of the average system queue backlog versus the average per-user throughput, for both the RA design and the AA design.

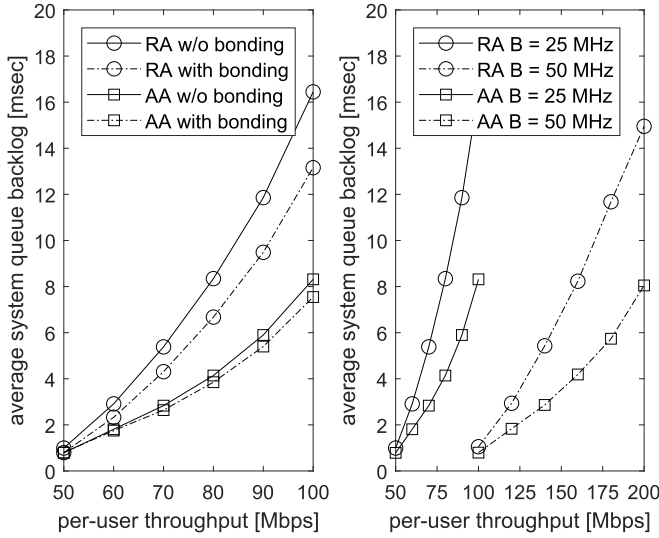


Fig. 2. The effect of bonding (left) and the effect of modulation bandwidth (right) on the performance of the average system queue backlog versus the average per-user throughput, for both the RA design and the AA design.

backlog versus the average per-user throughput, for both the RA design and the AA design. Again, it is clear that for both FoV settings of  $\text{FoV} = 90^\circ$  and  $\text{FoV} = 100^\circ$ , the AA design achieves a consistently shorter average system queue backlog than that of the RA design across all values of the average per-user throughput. Furthermore, for both the RA design and the AA design, increasing the FoV dramatically increases the average system queue backlog. This is indeed as expected, since the wider the FoV, the higher the interference level and the worse the average system queue backlog becomes, for both the RA design and the AA design.

3) *Effect of Channel Bonding*: The left subplot of Fig. 2 shows the effect of channel bonding on the performance of the average system queue backlog versus the average per-user throughput, for both the RA design and the AA design. Again, channel bonding refers to the scenario of supporting multi-AP

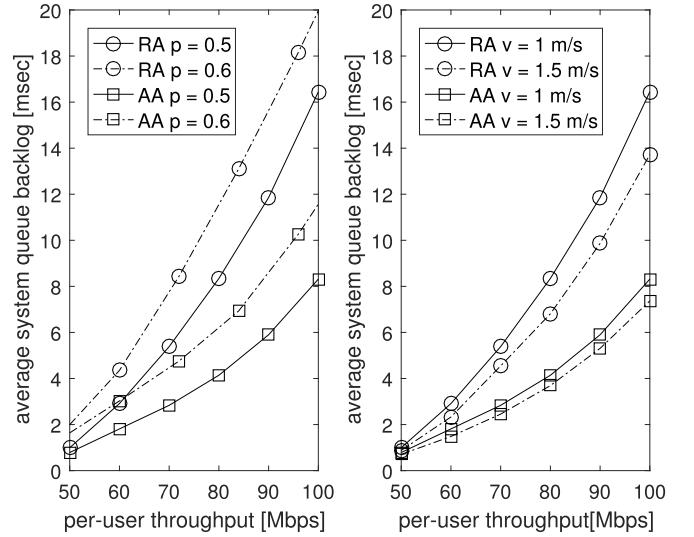


Fig. 3. The effect of Bernoulli mean (left) and the effect of walking speed (right) on the performance of the average system queue backlog versus the average per-user throughput, for both the RA design and the AA design.

association. In our simulations, we used  $N_k = |\mathcal{N}_{k,1}^{tw}|, \forall w, k$  for both the RA design and the AA design. It is clear that allowing multi-AP association noticeably decreases the average system queue backlog in the RA design. By contrast, only marginal improvements of the average system queue backlog can be observed, when channel bonding is employed in the AA design. This implies that the AA design is capable of exploiting the single-AP association, hence rendering channel bonding less attractive in the AA design.

4) *Effect of Modulation Bandwidth*: The right subplot of Fig. 2 shows the effect of the modulation bandwidth on the average system queue backlog versus the average per-user throughput, for both the RA design and the AA design. Again, it is clear that for both the modulation bandwidth settings of  $B = 25$  MHz and  $B = 50$  MHz, the AA design improves a consistently shorter average system queue backlog than that of the RA design across all values of the average per-user throughput. Furthermore, for both the RA design and the AA design, we observe a substantial impact of the modulation bandwidth on the performance of the average system queue backlog. More explicitly, as expected, at the same level of the average system queue backlog, doubling the modulation bandwidth from  $B = 25$  MHz to  $B = 50$  MHz roughly doubles the average per-user throughput, for both the RA design and the AA design.

5) *Effect of Bernoulli Mean*: The left subplot of Fig. 3 shows the effect of the Bernoulli mean on the average system queue backlog versus the average per-user throughput, for both the RA design and the AA design. Again, it is clear that for both the Bernoulli mean settings of  $p = 0.5$  and  $p = 0.6$ , the AA design improves a consistently shorter average system queue backlog than that of the RA design across all values of the average per-user throughput. Also as expected, for both the RA design and the AA design, the higher the Bernoulli mean, the higher the packet arrival rate and the higher the average system queue backlog.

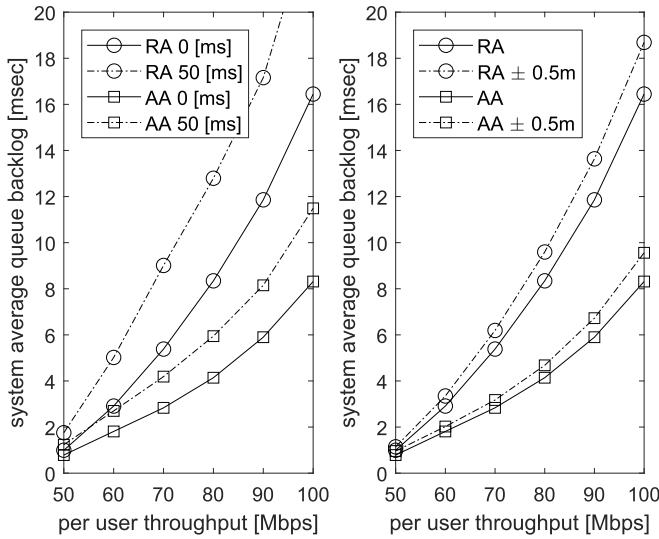


Fig. 4. The effect of association delay (left) and the effect of imperfect localization (right) on the performance of the average system queue backlog versus the average per-user throughput, for both the RA design and the AA design.

6) *Effect of Walking Speed:* The right subplot of Fig. 3 shows the effect of the walking speed on the average system queue backlog versus the average per-user throughput, for both the RA design and for the AA design. It is clear that for both velocities of  $v = 1$  [m/s] and  $v = 1.5$  [m/s], the AA design exhibits a consistently shorter average system queue backlog than that of the RA design across all values of the average per-user throughput. Interestingly, for both the RA design and the AA design, the higher the velocity, the shorter the average system queue backlog. Indeed, this is because the faster the users are moving, the more frequently the user will be served by strong LoS connections, hence leading to an *ergodic* experience. Should the users remain static all the time, the unlucky ones would always suffer from poor service and hence their average queue backlog would be increased.

7) *Effect of Association Delay:* The left subplot of Fig 4 shows the effect of the association delay at APs on the average system queue backlog versus the average per-user throughput, for both the RA design and the AA design. The association delay results into the outdated association decision. Fig 4 shows that as expected, this imperfection does impose a performance trade-off. Quantitatively, when the AA design is considered, at about 8 [ms] average system queue backlog, a loss of 10 [Mbps] average per-user throughput is observed owing to the association delay of 50 [ms] investigated. We believe that an association delay of 50 [ms] is quite a high value, which in turn implies that the design advocated is quite robust to this imperfection. However, different type of traffic distributions and user velocities would lead to different conclusions. Hence, appropriate counter-measures should be developed in the future.

8) *Effect of Imperfect Localization:* Fig 4 shows the effect of imperfect localization on the average system queue backlog versus the average per-user throughput, for both the RA design and the AA design. We model the imperfect localization by introducing uniformly distributed random positioning errors

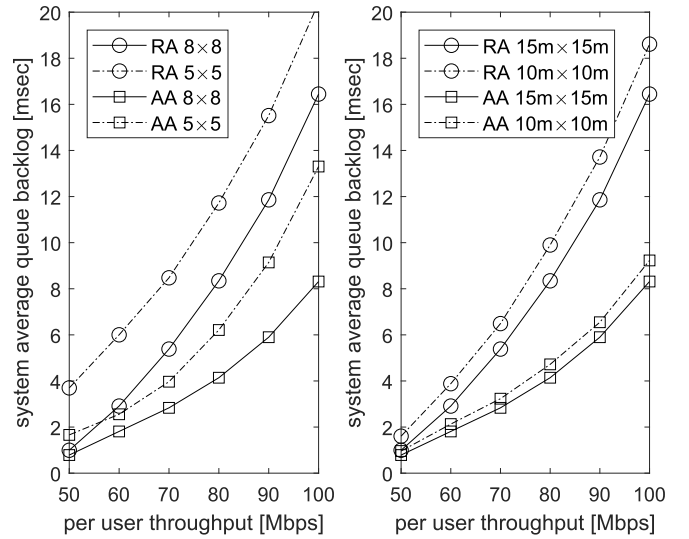


Fig. 5. The effect of reduced number of APs (left) and the effect of smaller rooms (right) on the performance of the average system queue backlog versus the average per-user throughput, for both the RA design and the AA design.

around the true value. The imperfect localization results into imperfect association decisions. Fig 4 shows that as expected, this imperfection does impose a performance degradation for both designs. We believe that limiting the positioning error to  $\pm 0.5$ m would be sufficient, noting that most of the positioning methods found in the literature are capable of achieving an accuracy at centi-meter level. This implies that the design advocated is quite robust to localization imperfections.

9) *Effect of Reduced Number of APs:* The left subplot of Fig 5 shows the effect of the reduced number of APs on the average system queue backlog versus the average per-user throughput, for both the RA design and the AA design. As expected, the performance degrades upon reducing the number of APs for both designs. This is because with fewer APs, fewer spatial resources will be available to share. Furthermore, with fewer APs, the chance of a particular user getting a LoS connection is reduced, hence typically only non-LoS links will be used. A further issue is that with fewer APs, the illumination density would not be uniform. Nevertheless, since VLC reuses the existing lighting infrastructure, a dense deployment would allow the best exploitation of spatial reuse. To this end, an interesting future direction would be to select the best subset of APs for lower complexity with minimal performance degradation.

10) *Effect of Smaller Room:* Fig 5 shows the effect of a smaller room on the average system queue backlog versus the average per-user throughput, for both the RA design and the AA design. To provide a fair comparison to the  $(8 \times 8)$  AP setting in the  $15 \times 15$  [m<sup>2</sup>] room with 20 users, we studied a  $(5 \times 5)$  AP setting in a  $10 \times 10$  [m<sup>2</sup>] room with 9 users. These two settings have similar AP density (number of APs per m<sup>2</sup>) and user density (number of users per m<sup>2</sup>). As expected, both settings exhibit similar performance trends. For smaller rooms, a slight performance degradation is observed for both designs, since stronger reflections are experienced and hence we have an increased crosstalk between users.

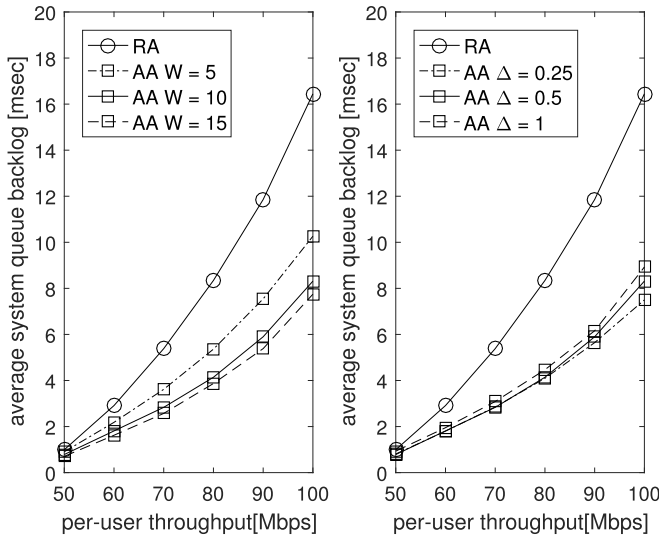


Fig. 6. The effect of prediction window size (left) and the effect of discretisation granularity (right) on the performance of the average system queue backlog versus the average per-user throughput, for the AA design.

11) *Effect of Prediction Window Size:* The left subplot of Fig. 6 shows the effect of the prediction window size on the average system queue backlog versus the average per-user throughput, for the AA design. It is clear that the average system queue backlog improves upon increasing the prediction window size from  $W = 5$  to  $W = 10$  and to  $W = 15$  at the cost of increasing the complexity, across all values of the average per-user throughput. Furthermore, the most noticeable improvement in the average system queue backlog appears upon increasing the prediction window size from  $W = 5$  to  $W = 10$ . Hence, it is important to strike a compromise between the performance and the complexity, although this aspect is beyond our current scope.

12) *Effect of Discretisation Granularity:* The right subplot of Fig. 6 shows the effect of the discretisation granularity on the average system queue backlog versus the average per-user throughput, for the AA design. As expected, the higher the discretisation granularity, the finer the continuous-valued queue backlog representation and the better the average system queue backlog becomes. Nevertheless, the differences in the average system queue backlog for  $\Delta = 0.25$ ,  $\Delta = 0.5$  and  $\Delta = 1$  remain quite small.

## V. CONCLUSIONS

In this paper, we provided a beneficial indoor VLC design for moving users and for dynamic wireless-traffic arrivals. A pair of location- and delay-aware association designs were investigated, namely the benchmarking RA design and the radical AA design. Efficient solutions were provided for both association designs and detailed optimisation algorithms were introduced. Our simulation results suggested that the AA design is capable of outperforming the RA design, resulting in a significantly better trade-off between the average system queue backlog and the average per-user throughput, for diverse parameter settings. Our study indicated that in indoor VLC, the system-wide average delay can be substantially reduced by taking advantage of the anticipatory approach

advocated. Finally, in our future work, it would be interesting to consider realistic positioning and tracking methods, hybrid user distributions, diverse mobility models, mixed wireless traffic profiles, joint uplink and downlink design, etc.

It is worth highlighting that our scheme would be challenged at high speeds. In this case, involving accurate positioning and tracking would become difficult, which in turn jeopardises the action of anticipation. In addition, the dwell time of the user would be too short to physically establish association, hence potentially leading to unnecessary association attempts. A potential solution in this case is to rely on a single anchor point for mobility control, namely to avoid frequent change of associations. For example, all APs could jointly serve as a single anchor, or the over-sailing radio connection could be in charge of the control plane in the context of HetNet. Nevertheless, this is certainly an interesting future research direction, especially in the case of having diverse velocities.

We consider downlink association in this paper, but naturally the location-awareness would rely on the existence of the uplink. In VLC, one could use the popular WiFi for the uplink. There has also been some prominent research [41], [42], including standardisation efforts dedicated to combining WiFi and VLC under the same 802 framework (IEEE 802.15 TG 7r1). Alternatively, one could rely on an Infra-red uplink dongle as implemented by PureLiFi (<https://purelifi.com/>). Indeed, bi-directional VLC systems have decoupled downlink and uplink. It will be thus interesting to study the ambitious closed-loop design in the future.

## APPENDIX

### OPTICAL-ELECTRONIC POWER CONVERSION

Since the primary purpose of LEDs is to provide illumination, the minimum required (maximum allowed) optical power  $P_{min}^{illu}$  ( $P_{max}^{illu}$ ) should satisfy the pre-defined illumination requirements constituted by the minimum illumination requirement  $\mathcal{I}_{min}$ , the maximum illumination requirement  $\mathcal{I}_{max}$  and the average illumination requirement  $\mathcal{I}_{avg}$ . Mathematically, we have to solve the problem of

$$P_{min}^{illu} = \min P \text{ or } P_{max}^{illu} = \max P, \quad (50)$$

$$\text{s.t. } \min_{\kappa \in [1, K_p]} \sum_n h_{\kappa, n}^{illu} LP \geq \mathcal{I}_{min}, \quad (51)$$

$$\max_{\kappa \in [1, K_p]} \sum_n h_{\kappa, n}^{illu} LP \leq \mathcal{I}_{max}, \quad (52)$$

$$\frac{1}{K_p} \sum_{\kappa} \sum_n h_{\kappa, n}^{illu} LP \in [\mathcal{I}_{avg}^-, \mathcal{I}_{avg}^+], \quad (53)$$

where  $\mathcal{I}_{avg}^+$  and  $\mathcal{I}_{avg}^-$  denote the  $\pm 5\%$  of  $\mathcal{I}_{avg}$ . Furthermore,  $h_{\kappa, n}^{illu}$  denotes the luminous flux of the unit optical power provided by the  $n$ th AP at the  $\kappa$ th point of the  $K_p$  equally partitioned receiver plane-tiles owing to the LoS propagation, which is given by

$$h_{\kappa, n}^{illu} = \frac{(m_L + 1)}{2\pi d^2 \xi} \cos^{m_L}(\theta) \cos(\psi), \quad (54)$$

where  $\xi$  denotes the optical power to luminous flux conversion factor [2], while  $m_L$ ,  $d$ ,  $\theta$  and  $\psi$  are defined similarly as in (1). In addition to satisfying the above illumination requirements,

the optical power  $P_o$  should also satisfy the per-LED dynamic range of  $[P_{min}, P_{max}]$ . As a result, by taking into account both the illumination requirements and the LED's physical limits, we have the constraint of

$$\max\{P_{min}^{illu}, P_{min}\} \leq P_o \leq \min\{P_{max}^{illu}, P_{max}\}. \quad (55)$$

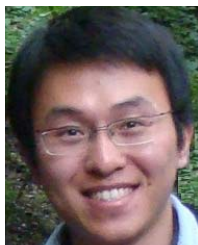
Furthermore, according to [29], the relationship between the electronic power  $\sigma_s^2$  and the optical power  $P_o$  is given by

$$P_o = \sigma_s \left[ \frac{1}{\sqrt{2\pi}} \exp\left(\frac{\check{\epsilon}^2}{\hat{\epsilon}^2}\right) - \check{\epsilon} f_Q(\check{\epsilon}) + \hat{\epsilon} f_Q(\hat{\epsilon}) \right] + P_{min}. \quad (56)$$

Hence, by opting for a desired optical power satisfying (55), we can find the electronic power  $\sigma_s^2$  used for communications.

## REFERENCES

- [1] R. Zhang, J. Wang, Z. Wang, Z. Xu, C. Zhao, and L. Hanzo, "Visible light communications in heterogeneous networks: Paving the way for user-centric design," *IEEE Wireless Commun.*, vol. 22, no. 2, pp. 8–16, Apr. 2015.
- [2] J. Grubor, S. Randel, K.-D. Langer, and J. Walewski, "Broadband information broadcasting using LED-based interior lighting," *J. Lightw. Technol.*, vol. 26, no. 24, pp. 3883–3892, Dec. 15, 2008.
- [3] A. H. Azhar, T. Tran, and D. O'Brien, "A gigabit/s indoor wireless transmission using MIMO-OFDM visible-light communications," *IEEE Photon. Technol. Lett.*, vol. 25, no. 2, pp. 171–174, Jan. 15, 2013.
- [4] D. Tsonev *et al.*, "Brien, "A 3-Gb/s single-LED OFDM-based wireless VLC link using a gallium nitride  $\mu$ LED," *IEEE Photon. Technol. Lett.*, vol. 26, no. 7, pp. 637–640, Apr. 1, 2014.
- [5] H. Haas, L. Yin, Y. Wang, and C. Chen, "What is LiFi?" *J. Lightw. Technol.*, vol. 34, no. 6, pp. 1533–1544, Mar. 15, 2016.
- [6] C. Chen, D. A. Basnayaka, and H. Haas, "Downlink performance of optical attocell networks," *J. Lightw. Technol.*, vol. 34, no. 1, pp. 137–156, Jan. 1, 2016.
- [7] R. Zhang, H. Claussen, H. Haas, and L. Hanzo, "Energy efficient visible light communications relying on amorphous cells," *IEEE J. Sel. Areas Commun.*, vol. 34, no. 2, pp. 894–906, Apr. 2016.
- [8] L. Chen, J. Wang, J. Zhou, D. W. K. Ng, R. Schober, and C. Zhao, "Distributed user-centric scheduling for visible light communication networks," *Opt. Exp.*, vol. 24, no. 14, pp. 15570–15589, 2016.
- [9] J. Armstrong, Y. A. Sekercioglu, and A. Neild, "Visible light positioning: A roadmap for international standardization," *IEEE Commun. Mag.*, vol. 51, no. 12, pp. 68–73, Dec. 2013.
- [10] T. Q. Wang, Y. A. Sekercioglu, A. Neild, and J. Armstrong, "Position accuracy of time-of-arrival based ranging using visible light with application in indoor localization systems," *J. Lightw. Technol.*, vol. 31, no. 20, pp. 3302–3308, Oct. 15, 2013.
- [11] H. Steendam, T. Q. Wang, and J. Armstrong, "Cramer-Rao bound for indoor visible light positioning using an aperture-based angular-diversity receiver," in *Proc. IEEE Int. Conf. Commun. (ICC)*, May 2016, pp. 1–6.
- [12] Y. Cui, V. K. N. Lau, R. Wang, H. Huang, and S. Zhang, "A survey on delay-aware resource control for wireless systems—Large deviation theory, stochastic Lyapunov drift, and distributed stochastic learning," *IEEE Trans. Inf. Theory*, vol. 58, no. 3, pp. 1677–1701, Mar. 2012.
- [13] L. Georgiadis, M. J. Neely, and L. Tassiulas, "Resource allocation and cross-layer control in wireless networks," *Found. Trends Netw.*, vol. 1, no. 1, pp. 1–144, 2006.
- [14] V. K. N. Lau and Y. Cui, "Delay-optimal power and subcarrier allocation for OFDMA systems via stochastic approximation," *IEEE Trans. Wireless Commun.*, vol. 9, no. 1, pp. 227–233, Jan. 2010.
- [15] N. Bui, M. Cesana, S. A. Hosseini, Q. Liao, I. Malanchini, and J. Widmer, "A survey of anticipatory mobile networking: Context-based classification, prediction methodologies, and optimization techniques," *IEEE Commun. Surveys Tuts.*, vol. 19, no. 3, pp. 1790–1821, 2017.
- [16] R. Margolies *et al.*, "Exploiting mobility in proportional fair cellular scheduling: Measurements and algorithms," *IEEE/ACM Trans. Netw.*, vol. 24, no. 1, pp. 355–367, Feb. 2016.
- [17] H. Abou-Zeid, H. S. Hassanein, and S. Valentin, "Energy-efficient adaptive video transmission: Exploiting rate predictions in wireless networks," *IEEE Trans. Veh. Technol.*, vol. 63, no. 5, pp. 2013–2026, Jun. 2014.
- [18] J. Tadrous, A. Eryilmaz, and H. El Gamal, "Proactive resource allocation: Harnessing the diversity and multicast gains," *IEEE Trans. Inf. Theory*, vol. 59, no. 8, pp. 4833–4854, Aug. 2013.
- [19] E. Bastug, M. Bennis, and M. Debbah, "Living on the edge: The role of proactive caching in 5G wireless networks," *IEEE Commun. Mag.*, vol. 52, no. 8, pp. 82–89, Aug. 2014.
- [20] Z. R. Zaidi and B. L. Mark, "Real-time mobility tracking algorithms for cellular networks based on Kalman filtering," *IEEE Trans. Mobile Comput.*, vol. 4, no. 2, pp. 195–208, Mar. 2005.
- [21] R. Xu and D. Wunsch, II, "Survey of clustering algorithms," *IEEE Trans. Neural Netw.*, vol. 16, no. 3, pp. 645–678, May 2005.
- [22] M. Kasparick, R. L. G. Cavalcante, S. Valentin, S. Stańczak, and M. Yukawa, "Kernel-based adaptive online reconstruction of coverage maps with side information," *IEEE Trans. Veh. Technol.*, vol. 65, no. 7, pp. 5461–5473, Jul. 2016.
- [23] L. S. Muppirisetty, T. Svensson, and H. Wymeersch, "Spatial wireless channel prediction under location uncertainty," *IEEE Trans. Wireless Commun.*, vol. 15, no. 2, pp. 1031–1044, Feb. 2016.
- [24] C. Chen, X. Zhu, G. de Veciana, A. C. Bovik, and R. W. Heath, Jr., "Rate adaptation and admission control for video transmission with subjective quality constraints," *IEEE J. Sel. Topics Signal Process.*, vol. 9, no. 1, pp. 22–36, Feb. 2015.
- [25] S. J. Qin and T. A. Badgwell, "A survey of industrial model predictive control technology," *Control Eng. Pract.*, vol. 11, no. 7, pp. 733–764, 2003.
- [26] C. Chen, R. W. Heath, Jr., A. C. Bovik, and G. de Veciana, "A Markov decision model for adaptive scheduling of stored scalable videos," *IEEE Trans. Circuits Syst. Video Technol.*, vol. 23, no. 6, pp. 1081–1095, Jun. 2013.
- [27] G. P. Fettweis, "The tactile Internet: Applications and challenges," *IEEE Veh. Technol. Mag.*, vol. 9, no. 1, pp. 64–70, Mar. 2014.
- [28] T. Komine and M. Nakagawa, "Fundamental analysis for visible-light communication system using LED lights," *IEEE Trans. Consum. Electron.*, vol. 50, no. 1, pp. 100–107, Feb. 2004.
- [29] S. Dimitrov, S. Sinanovic, and H. Haas, "Clipping noise in OFDM-based optical wireless communication systems," *IEEE Trans. Commun.*, vol. 60, no. 4, pp. 1072–1081, Apr. 2012.
- [30] A. L. Stolyar and K. Ramanan, "Largest weighted delay first scheduling: Large deviations and optimality," *Ann. Appl. Probab.*, vol. 11, no. 1, pp. 1–48, 2001.
- [31] M. Yang, K. Jung, A. Park, and S.-H. Kim, "Definitive link layer triggers for predictive handover optimization," in *Proc. IEEE Veh. Technol. Conf. (VTC Spring)*, May 2008, pp. 2326–2330.
- [32] S.-J. Yoo, D. Cypher, and N. Golmie, "Predictive handover mechanism based on required time estimation in heterogeneous wireless networks," in *Proc. IEEE Military Commun. Conf. (MILCOM)*, Nov. 2008, pp. 1–7.
- [33] R. Bellman, *Dynamic Programming*, 1st ed. Princeton, NJ, USA: Princeton Univ. Press, 1957.
- [34] D. P. Bertsekas, *Dynamic Programming and Optimal Control*, 2nd ed. Belmont, MA, USA: Athena Scientific, 2000.
- [35] D. Adelman and A. J. Mersereau, "Relaxations of weakly coupled stochastic dynamic programs," *Oper. Res.*, vol. 56, no. 3, pp. 712–727, 2008.
- [36] W. B. Powell, *Approximate Dynamic Programming: Solving the Curses of Dimensionality* (Wiley Series in Probability and Statistics). Hoboken, NJ, USA: Wiley, 2007.
- [37] H. Topaloglu and S. Kunnunkal, "Approximate dynamic programming methods for an inventory allocation problem under uncertainty," *Naval Res. Logistics*, vol. 53, no. 8, pp. 822–841, 2006.
- [38] J. M. Nascimento and W. B. Powell, "An optimal approximate dynamic programming algorithm for the lagged asset acquisition problem," *Math. Oper. Res.*, vol. 34, no. 1, pp. 210–237, 2009.
- [39] F. Fu and M. van der Schaar, "A systematic framework for dynamically optimizing multi-user wireless video transmission," *IEEE J. Sel. Areas Commun.*, vol. 28, no. 3, pp. 308–320, Apr. 2010.
- [40] J. L. Williams, J. W. Fisher, III, and A. S. Willsky, "Approximate dynamic programming for communication-constrained sensor network management," *IEEE Trans. Signal Process.*, vol. 55, no. 8, pp. 4300–4311, Aug. 2007.
- [41] M. Ayyash *et al.*, "Coexistence of WiFi and LiFi toward 5G: Concepts, opportunities, and challenges," *IEEE Commun. Mag.*, vol. 54, no. 2, pp. 64–71, Feb. 2016.
- [42] S. Naribole, S. Chen, E. Heng, and E. Knightly, "LiRa: A WLAN architecture for visible light communication with a Wi-Fi uplink," in *Proc. 14th Annu. IEEE Int. Conf. Sens., Commun., Netw. (SECON)*, Jun. 2017, pp. 1–9.



**Rong Zhang** (M'09–SM'16) received the Ph.D. degree in wireless communications from the University of Southampton (UoS) in 2009. He was a Research Assistant with the Mobile Virtual Centre of Excellence, UoS, one of the U.K.'s largest industrial-academic partnerships in ICT. He is currently an Assistant Professor in the Southampton Wireless Group, School of Electronics and Computer Science, UoS. During his post-doctoral period in ECS, he contributed as the UoS lead researcher on a number of international projects. After that, he took

his industrial consulting leave for Huawei EU Research and Development as a System Algorithms Expert. He has over 90 IEEE/OSA publications, including over 60 journals (over 20 of which as first author). He was the recipient of the prestigious Dean's Publication Award. He is also the recipient of the prestigious RAEng Industrial Fellowship. He regularly serves as an editor/reviewer for IEEE/OSA journals and as a reviewer/panelist for funding bodies. He has served several times as a TPC member/invited session chair of major conferences. He is a RAEng Industrial Fellow, a member of the OSA, and a member of the HEA.



**Ying Cui** received the B.E. degree in electronic and information engineering from Xi'an Jiao Tong University, China, in 2007, and the Ph.D. degree in electronic and computer engineering from The Hong Kong University of Science and Technology, Hong Kong, in 2011. In 2011, she was a Visiting Assistant in Research in the Department of Electrical Engineering, Yale University, USA. In 2012, she was a Visiting Scholar in the Department of Electronic Engineering, Macquarie University, Australia. From 2012 to 2013, she was a Post-Doctoral Research

Associate in the Department of Electrical and Computer Engineering, Northeastern University, USA. From 2013 to 2014, she was a Post-Doctoral Research Associate in the Department of Electrical Engineering and Computer Science, Massachusetts Institute of Technology, USA. Since 2015, she has been an Associate Professor in the Department of Electronic Engineering, Shanghai Jiao Tong University, China. Her current research interests include cache-enabled wireless networks, future Internet architecture, delay-sensitive cross-layer control and network coding. She was selected into China's 1000 Plan Program for Young Talents in 2013. She received the Best Paper Award at the IEEE ICC, London, U.K., 2015.



**Holger Claussen** (SM'10) received the Ph.D. degree in signal processing for digital communications from the University of Edinburgh, U.K., in 2004. He was the Head of the Autonomous Networks and Systems Research Department, Bell Labs, where he directed research in the area of self-managing networks to enable the first large scale femtocell deployments from 2009 onward. He is currently the Leader of the Small Cells Research Department, Nokia Bell Labs, Ireland and USA. In this role, he and his team are innovating in all areas related to future evolution,

deployment, and operation of small cell networks to enable exponential growth in mobile data traffic. He has authored one book, over 110 publications, and 120 filed patent families. His research in this domain has been commercialized in Nokia's small cell product portfolio and continues to have significant impact. He received the 2014 World Technology Award in the individual category communications technologies for innovative work of the greatest likely long-term significance. He joined Bell Labs in 2004, where he began his research in the areas of network optimization, cellular architectures, and improving energy efficiency of networks. He is Fellow of the World Technology Network and member of the IET.



**Harald Haas** (F'17) received the Ph.D. degree from the University of Edinburgh in 2001. He currently holds the Chair of Mobile Communications at the University of Edinburgh. He is also the Founder and Chief Scientific Officer of pureLiFi Ltd. and the Director of the LiFi Research and Development Center, University of Edinburgh. He has published over 400 conference and journal papers including a paper in *Science*. His main research interests are in LiFi and visible light communications. He first introduced and coined spatial modulation and LiFi.

The latter was listed among the 50 best inventions in TIME Magazine 2011. He was an invited speaker at TED Global 2011, and his talk "Wireless Data from Every Light Bulb" has been watched online over 2.5 million times. He gave a second TED Global Lecture in 2015 on the use of solar cells as LiFi data detectors and energy harvesters. This has been viewed online over 2 million times. He was elected a Fellow of the Royal Society of Edinburgh in 2017. He was co-recipient of recent Best Paper Awards at VTC-Fall, 2013, VTC-Spring 2015, ICC 2016, and ICC 2017. He was co-recipient of the EURASIP Best Paper Award for the *Journal on Wireless Communications and Networking* in 2015, and a co-recipient of the Jack Neubauer Memorial Award of the IEEE Vehicular Technology Society. In 2012 and 2017, he was the recipient of the prestigious Established Career Fellowship from the Engineering and Physical Sciences Research Council (EPSRC) within Information and Communications Technology, U.K. In 2014, he was selected by EPSRC as one of ten Recognizing Inspirational Scientists and Engineers (RISE) Leaders in the U.K. In 2016, he received the Outstanding Achievement Award from the International Solid State Lighting Alliance. He is an Editor of the IEEE TRANSACTIONS ON COMMUNICATIONS and the IEEE JOURNAL OF LIGHTWAVE TECHNOLOGIES.



**Lajos Hanzo** received the D.Sc. degree in electronics in 1976 and the Ph.D. degree in 1983. During his 40-year career in telecommunications he has held various research and academic posts in Hungary, Germany, and U.K. Since 1986, he has been with the School of Electronics and Computer Science, University of Southampton, U.K. He is currently directing a 60-strong academic research team, working on a range of research projects in the field of wireless multimedia communications sponsored by industry, the Engineering and Physical Sciences

Research Council, U.K., the European Research Council's Advanced Fellow Grant, and the Royal Society's Wolfson Research Merit Award. He is an enthusiastic supporter of industrial and academic liaison and he offers a range of industrial courses. He has successfully supervised 111 Ph.D. students, co-authored 18 John Wiley/IEEE Press books on mobile radio communications totaling in excess of 10 000 pages, and published 1703 research contributions on IEEE Xplore. He has over 30 000 citations and an H-index of 72. He is a fellow, FREng, and FIET of EURASIP. He received an Honorary Doctorate from the Technical University of Budapest in 2009 and The University of Edinburgh in 2015. In 2016, he was admitted to the Hungarian Academy of Science. He is a Governor of the IEEE VTS. He has served as the TPC chair and general chair of IEEE conferences, presented keynote lectures and has received a number of distinctions. He is the Chair in Telecommunications with the University of Southampton. From 2008 to 2012, he was an Editor-in-Chief of the IEEE Press and a Chaired Professor also at Tsinghua University, Beijing.